www.sciencemag.org/cgi/content/full/science.aar7797/DC1

Supplementary Material for

Building one molecule from a reservoir of two atoms

L. R. Liu, J. D. Hood, Y. Yu, J. T. Zhang, N. R. Hutzler, T. Rosenband, K.-K. Ni*

*Corresponding author. E-mail: ni@chemistry.harvard.edu

Published 12 April 2018 as *Science* First Release
DOI: 10.1126/science.aar7797

This PDF file includes:

Other Supplementary Material for this manuscript includes the following:
(available at www.sciencemag.org/content/science.aar7797/DC1)

Table S1 as a separate .txt file

MATERIALS AND METHODS

Experimental apparatus

All experiments are performed in an epoxy-bonded quartz vacuum chamber maintained at $< 10^{-8}$ Pa by a getter/ion pump. Six alkali dispensers for Cs and Na are suspended inside the chamber, 5 inches from the MOT region. We maintain a constant current of 2A and 4 A through two of them to maintain sufficient Cs and Na vapor pressures the experiments presented.

The 700 nm optical tweezer is derived from a cavity-locked Titanium sapphire laser. The 976 nm tweezer is derived from a free-running distributed Bragg reflector (DBR) laser.

The light for the Na MOT is derived from a frequency doubled Raman fiber amplifier that is seeded by a 1178 nm external cavity diode laser (ECDL). The cooling and the repumping frequencies are generated from the same laser by sending it through a 1.7 GHz acousto optical modulator. Optical pumping for Na is provided by another 1178 nm ECDL that is frequency doubled with a PPLN waveguide. Optical pumping on the D1 instead of D2 line is necessary to avoid unwanted off-resonant cycling transitions in the Na D2 line due to the small excited-state hyperfine splitting. All lasers for Na are locked via saturated absorption spectroscopy to a vapor cell.

The light for the Cs MOT is derived from two 852 nm DBR lasers. The first is locked to the Cs D2 line via saturated absorption spectroscopy, while the second is referenced to the first with a phase lock, providing repumping and cooling frequencies respectively. Optical pumping for Cs is provided by the same light.

At the vacuum chamber, 2 mW of Cs MOT and 5 mW of Na MOT light are expanded to 6 mm beam diameter and combined before being directed into the chamber in a 6-beam configuration. The gradient field for both MOTs, which are formed simultaneously, is 9 G/cm. A 0.55 NA achromatic objective points at the chamber from between two of the horizontal MOT beams. A custom dichroic separates resonant fluorescence from the far detuned tweezers for both species simultaneously.

We image atoms onto an EMCCD with a magnification factor of 16. The total efficiency from atomic fluorescence to photoelectron counts is about 4%. To determine the presence of atoms, we image them with resonant light. The signal is $\sim 10^4$ counts/s, at imaging times of 1 ms and 10 ms for Na and Cs respectively.

Na and Cs effective pair density

The "effective pair density" n_2 is defined as the probability of finding a single Na and Cs atom per unit volume (eq. S1)

$$n_2 = \int_{-\infty}^{\infty}\int_{-\infty}^{\infty}\int_{-\infty}^{\infty} n_{Cs}(x,y,z) n_{Na}(x,y,z)\,\mathrm{d}x\,\mathrm{d}y\,\mathrm{d}z \tag{S1}$$

To get the individual atomic density distributions $n_{Na}(x,y,z)$ and $n_{Cs}(x,y,z)$, we assumed the atoms occupy a thermal ensemble in a 3-dimensional harmonic oscillator potential with trap frequencies (132, 123, 24) kHz for Na and (150, 140, 28) kHz for Cs, as measured by parametric heating. The temperature during the collision measurements was measured by a release and recapture technique (***?***) and found to be 90 μK and 42 μK for Cs and Na, respectively, giving $n_2 = 2 \times 10^{12}\,\mathrm{cm}^{-3}$. For the PA measurements the Cs temperature was 28 μK, giving $n_2 = 3 \times 10^{12}\,\mathrm{cm}^{-3}$.

Na and Cs 1- and 2-body collisions

To obtain the fits in Fig. 3, we use the model depicted in Fig. S1. This yields the system of differential equations eq. S2 for the time dependence of each tweezer occupation state. The boundary conditions are the initial populations of each state (which can be read off directly from the data) and the fact that all population should end up in (0,0) at long times.

Single atom images and post-selection allow us to isolate individual branches of Fig. S1. The 1-body processes ((1,0) to (0,0) and (0,1) to (0,0)) feature only a single exponential decay and are fitted first to obtain $1/k_{Cs} = 5.3(1)\,\mathrm{s}$ and $1/k_{Na} = 5.1(3)\,\mathrm{s}$, (Fig. 3, Right). These rates are then fixed and the losses out of (1,1;L) are fitted to obtain $1/k_{2s} = 0.63(1)$ s (Fig. 3, Center). Finally, this rate is fixed as well and the losses out of (1,1;M) are fitted to obtain $1/k_{2f} = 8(1)$ ms (Fig. 3, Left).

$$\frac{d}{dt}\begin{bmatrix} P_{00}(t) \\ P_{01}(t) \\ P_{10}(t) \\ P_{11;L}(t) \\ P_{11;M}(t) \end{bmatrix} = \begin{bmatrix} 0 & k_{Na} & k_{Cs} & k_{2s} & k_{2f} \\ 0 & -k_{Na} & 0 & k_{Cs} & k_{Cs} \\ 0 & 0 & -k_{Cs} & k_{Na} & k_{Na} \\ 0 & 0 & 0 & -k_{2s} - k_{Cs} - k_{Na} & 0 \\ 0 & 0 & 0 & 0 & -k_{2f} - k_{Cs} - k_{Na} \end{bmatrix} \begin{bmatrix} P_{00}(t) \\ P_{01}(t) \\ P_{10}(t) \\ P_{11;L}(t) \\ P_{11;M}(t) \end{bmatrix} \tag{S2}$$

For the measurements of 2-body collisions, the Cs and Na temperatures are measured to be 90 μK and 42 μK respectively, giving $n_2 = 2.3 \times 10^{12}\,\mathrm{cm}^{-3}$. This yields a loss rate constant $\beta = 5 \times 10^{-11}\,\mathrm{cm}^3/\mathrm{s}$.

NaCs* Photoassociation spectroscopy

The NaCs photoassociation spectroscopy data presented in Fig. 4 are tabulated in Table_S1.txt. The data are organized in columns. The first column is the PA laser detuning in GHz. The next columns are probability, followed by associated error bar, for the outcomes (Cs,Na) = (1,1) to (0,0), (1,1) to (0,1), (1,1) to (1,0), (1,1) to (1,1), (0,1) to (0,0), and (1,0) to (0,0).

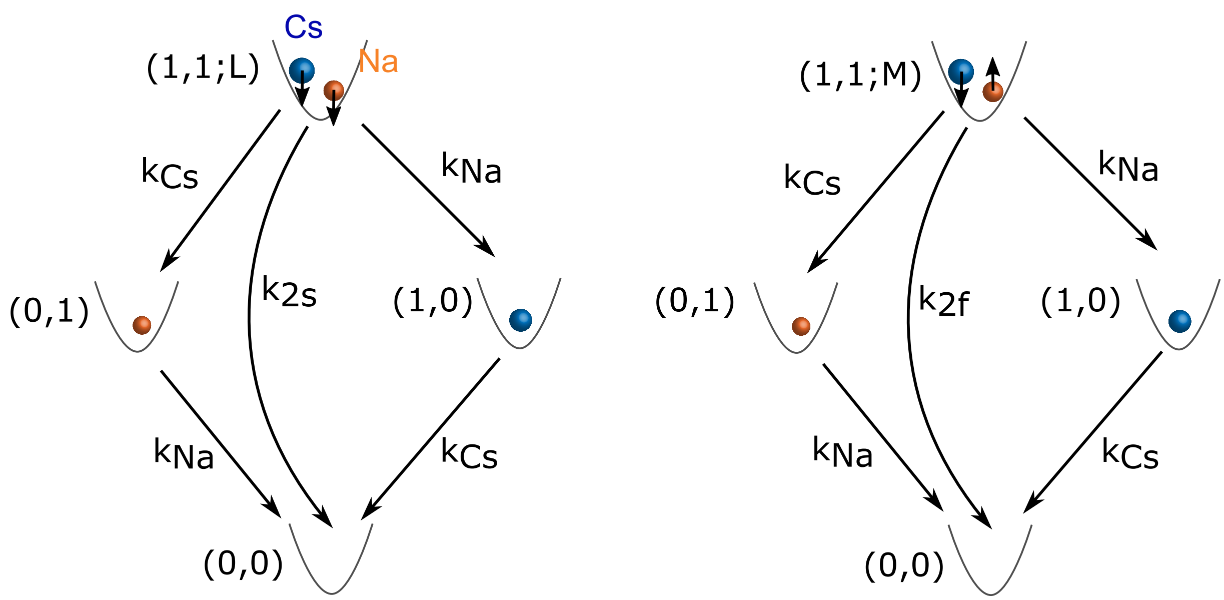

Figure S1: **Model for 2-body collisions of Na and Cs.** Four possible tweezer occupation states exist: (1,1) both Cs and Na; (0,1) only Na; (1,0) only Cs; (0,0) empty. Transitions between states are depicted by arrows with associated rates: 1-body Cs loss k_{Cs}, 1-body Na loss k_{Na}, slow 2-body loss k_{2s}, fast 2-body loss k_{2f}. Single atom images allow us to directly detect transitions between any two of these states, thereby determining the rates k. (1,1) is further split into two components: L, where both Na and Cs are in their lowest hyperfine states; and M, any other combination of hyperfine states.

References and Notes

1. D. R. Herschbach, Molecular Dynamics of Elementary Chemical Reactions(Nobel Lecture). *Angew. Chem. Int. Ed. Engl.* **26**, 1221–1243 (1987). doi:10.1002/anie.198712211

2. Y. T. Lee, Molecular Beam Studies of Elementary Chemical Processes(Nobel Lecture). *Angew. Chem. Int. Ed. Engl.* **26**, 939–951 (1987). doi:10.1002/anie.198709393

3. A. B. Henson, S. Gersten, Y. Shagam, J. Narevicius, E. Narevicius, Observation of resonances in Penning ionization reactions at sub-kelvin temperatures in merged beams. *Science* **338**, 234–238 (2012). doi:10.1126/science.1229141 Medline

4. W. E. Perreault, N. Mukherjee, R. N. Zare, Quantum control of molecular collisions at 1 kelvin. *Science* **358**, 356–359 (2017). doi:10.1126/science.aao3116 Medline

5. S. Ospelkaus, K.-K. Ni, D. Wang, M. H. G. de Miranda, B. Neyenhuis, G. Quéméner, P. S. Julienne, J. L. Bohn, D. S. Jin, J. Ye, Quantum-state controlled chemical reactions of ultracold potassium-rubidium molecules. *Science* **327**, 853–857 (2010). doi:10.1126/science.1184121 Medline

6. K.-K. Ni, S. Ospelkaus, D. Wang, G. Quéméner, B. Neyenhuis, M. H. G. de Miranda, J. L. Bohn, J. Ye, D. S. Jin, Dipolar collisions of polar molecules in the quantum regime. *Nature* **464**, 1324–1328 (2010). doi:10.1038/nature08953 Medline

7. M. H. G. de Miranda, A. Chotia, B. Neyenhuis, D. Wang, G. Quéméner, S. Ospelkaus, J. L. Bohn, J. Ye, D. S. Jin, Controlling the quantum stereodynamics of ultracold bimolecular reactions. *Nat. Phys.* **7**, 502–507 (2011). doi:10.1038/nphys1939

8. K. Liu, CROSSED-bEAM STUDIES OF nEUTRAL rEACTIONS: State-specific differential cross sections. *Annu. Rev. Phys. Chem.* **52**, 139–164 (2001). doi:10.1146/annurev.physchem.52.1.139 Medline

9. X. Yang, State-to-state dynamics of elementary bimolecular reactions. *Annu. Rev. Phys. Chem.* **58**, 433–459 (2007). doi:10.1146/annurev.physchem.58.032806.104632 Medline

10. A. Klein, Y. Shagam, W. Skomorowski, P. S. Żuchowski, M. Pawlak, L. M. C. Janssen, N. Moiseyev, S. Y. T. van de Meerakker, A. van der Avoird, C. P. Koch, E. Narevicius, Directly probing anisotropy in atom–molecule collisions through quantum scattering resonances. *Nat. Phys.* **13**, 35–38 (2016). doi:10.1038/nphys3904

11. L. Ratschbacher, C. Zipkes, C. Sias, M. Köhl, Controlling chemical reactions of a single particle. *Nat. Phys.* **8**, 649–652 (2012). doi:10.1038/nphys2373

12. S. A. Moses, J. P. Covey, M. T. Miecnikowski, B. Yan, B. Gadway, J. Ye, D. S. Jin, Creation of a low-entropy quantum gas of polar molecules in an optical lattice. *Science* **350**, 659–662 (2015). doi:10.1126/science.aac6400 Medline

13. P. Puri, M. Mills, C. Schneider, I. Simbotin, J. A. Montgomery Jr., R. Côté, A. G. Suits, E. R. Hudson, Synthesis of mixed hypermetallic oxide $BaOCa^+$ from laser-cooled reagents in an atom-ion hybrid trap. *Science* **357**, 1370–1375 (2017). doi:10.1126/science.aan4701 Medline

14. D. M. Eigler, E. K. Schweizer, Positioning single atoms with a scanning tunnelling microscope. *Nature* **344**, 524–526 (1990). doi:10.1038/344524a0

15. P. J. Dagdigian, L. Wharton, Molecular Beam Electric Deflection and Resonance Spectroscopy of the Heteronuclear Alkali Dimers: ^{39}K ^{7}Li, Rb ^{7}Li, ^{39}K ^{23}Na, Rb ^{23}Na, and ^{133}Cs ^{23}Na. *J. Chem. Phys.* **57**, 1487–1496 (1972). doi:10.1063/1.1678429

16. N. Schlosser, G. Reymond, I. Protsenko, P. Grangier, Sub-poissonian loading of single atoms in a microscopic dipole trap. *Nature* **411**, 1024–1027 (2001). doi:10.1038/35082512 Medline

17. M. S. Safronova, B. Arora, C. W. Clark, Frequency-dependent polarizabilities of alkali-metal atoms from ultraviolet through infrared spectral regions. *Phys. Rev. A* **73**, 022505 (2006). doi:10.1103/PhysRevA.73.022505

18. A. Fuhrmanek, R. Bourgain, Y. R. P. Sortais, A. Browaeys, Light-assisted collisions between a few cold atoms in a microscopic dipole trap. *Phys. Rev. A* **85**, 062708 (2012). doi:10.1103/PhysRevA.85.062708

19. P. Sompet, A. V. Carpentier, Y. H. Fung, M. McGovern, M. F. Andersen, Dynamics of two atoms undergoing light-assisted collisions in an optical microtrap. *Phys. Rev. A* **88**, 051401 (2013). doi:10.1103/PhysRevA.88.051401

20. N. R. Hutzler, L. R. Liu, Y. Yu, K.-K. Ni, Eliminating light shifts for single atom trapping. *New J. Phys.* **19**, 023007 (2017). doi:10.1088/1367-2630/aa5a3b

21. J. Beugnon, C. Tuchendler, H. Marion, A. Gaëtan, Y. Miroshnychenko, Y. R. P. Sortais, A. M. Lance, M. P. A. Jones, G. Messin, A. Browaeys, P. Grangier, Two-dimensional transport and transfer of a single atomic qubit in optical tweezers. *Nat. Phys.* **3**, 696–699 (2007). doi:10.1038/nphys698

22. A. M. Kaufman, B. J. Lester, C. M. Reynolds, M. L. Wall, M. Foss-Feig, K. R. A. Hazzard, A. M. Rey, C. A. Regal, Two-particle quantum interference in tunnel-coupled optical tweezers. *Science* **345**, 306–309 (2014). doi:10.1126/science.1250057 Medline

23. B. Ueberholz, S. Kuhr, D. Frese, D. Meschede, V. Gomer, Counting cold collisions. *J. Phys. At. Mol. Opt. Phys.* **33**, L135–L142 (2000). doi:10.1088/0953-4075/33/4/105

24. Materials and methods are available as supplementary materials.

25. R. A. Cline, J. D. Miller, M. R. Matthews, D. J. Heinzen, Spin relaxation of optically trapped atoms by light scattering. *Opt. Lett.* **19**, 207 (1994). doi:10.1364/OL.19.000207 Medline

26. K. M. Jones, E. Tiesinga, P. D. Lett, P. S. Julienne, Ultracold photoassociation spectroscopy: Long-range molecules and atomic scattering. *Rev. Mod. Phys.* **78**, 483–535 (2006). doi:10.1103/RevModPhys.78.483

27. M. Korek, S. Bleik, A. R. Allouche, Theoretical calculation of the low laying electronic states of the molecule NaCs with spin-orbit effect. *J. Chem. Phys.* **126**, 124313 (2007). doi:10.1063/1.2710257 Medline

28. A. Grochola, P. Kowalczyk, J. Szczepkowski, W. Jastrzebski, A. Wakim, P. Zabawa, N. P. Bigelow, Spin-forbidden c 3 Σ + (Ω = 1) ⟵ X 1 Σ + transition in NaCs: Investigation of the Ω = 1 state in hot and cold environments. *Phys. Rev. A* **84**, 012507 (2011). doi:10.1103/PhysRevA.84.012507

29. R. J. LeRoy, R. B. Bernstein, Dissociation energy and long-range potential of diatomic molecules from vibrational spacings of higher levels. *J. Chem. Phys.* **52**, 3869–3879 (1970). doi:10.1063/1.1673585

30. M. Marinescu, H. Sadeghpour, Long-range potentials for two-species alkali-metal atoms. *Phys. Rev. A* **59**, 390–404 (1999). doi:10.1103/PhysRevA.59.390

31. A. Grochola, P. Kowalczyk, W. Jastrzebski, Investigation of the B1Π state in NaCs by polarisation labelling spectroscopy. *Chem. Phys. Lett.* **497**, 22–25 (2010). doi:10.1016/j.cplett.2010.07.093

32. K. Bergmann, H. Theuer, B. W. Shore, Coherent population transfer among quantum states of atoms and molecules. *Rev. Mod. Phys.* **70**, 1003–1025 (1998). doi:10.1103/RevModPhys.70.1003

33. L. R. Liu *et al*., *ArXiv:1701.03121* (2017).

34. C. Monroe, D. M. Meekhof, B. E. King, S. R. Jefferts, W. M. Itano, D. J. Wineland, P. Gould, Resolved-sideband Raman cooling of a bound atom to the 3D zero-point energy. *Phys. Rev. Lett.* **75**, 4011–4014 (1995). doi:10.1103/PhysRevLett.75.4011 Medline

35. X. Li, T. A. Corcovilos, Y. Wang, D. S. Weiss, 3D projection sideband cooling. *Phys. Rev. Lett.* **108**, 103001 (2012). doi:10.1103/PhysRevLett.108.103001 Medline

36. A. M. Kaufman, B. J. Lester, C. A. Regal, Cooling a Single Atom in an Optical Tweezer to Its Quantum Ground State. *Phys. Rev. X* **2**, 041014 (2012). doi:10.1103/PhysRevX.2.041014

37. Y. Yu *et al*., *ArXiv:1708.03296* (2017).

38. D. Barredo, S. de Léséleuc, V. Lienhard, T. Lahaye, A. Browaeys, An atom-by-atom assembler of defect-free arbitrary two-dimensional atomic arrays. *Science* **354**, 1021–1023 (2016). doi:10.1126/science.aah3778 Medline

39. M. Endres, H. Bernien, A. Keesling, H. Levine, E. R. Anschuetz, A. Krajenbrink, C. Senko, V. Vuletic, M. Greiner, M. D. Lukin, Atom-by-atom assembly of defect-free one-dimensional cold atom arrays. *Science* **354**, 1024–1027 (2016). doi:10.1126/science.aah3752 Medline

40. D. DeMille, Quantum computation with trapped polar molecules. *Phys. Rev. Lett.* **88**, 067901 (2002). doi:10.1103/PhysRevLett.88.067901 Medline

41. N. Y. Yao, M. P. Zaletel, D. M. Stamper-Kurn, A. Vishwanath, *arXiv preprint arXiv:1510.06403* (2015).

42. B. Sundar, B. Gadway, K. R. Hazzard, *arXiv preprint arXiv:1708.02112* (2017).

43. C. Tuchendler, A. M. Lance, A. Browaeys, Y. R. Sortais, P. Grangier, Energy distribution and cooling of a single atom in an optical tweezer. *Phys. Rev. A* **78**, 033425 (2008). doi:10.1103/PhysRevA.78.033425